Vinylene carbonate and vinylene trithiocarbonate as electrolyte additives for lithium ion battery

Chia-Chin Chang [a,*], Sheng-Hsiang Hsu [a], Yi-Fang Jung [b], Chien-Hsin Yang [c]

[a] Department of Greenergy, National University of Tainan, Tainan 70101, Taiwan
[b] Department of Material Science, National University of Tainan, Tainan 70101, Taiwan
[c] Department of Chemical and Materials Engineering, National University of Kaohsiung, Kaohsiung 811, Taiwan

ABSTRACT

Vinylene carbonate (VC) and vinylene trithiocarbonate (VTC) are studied as electrolyte additives in two kinds of electrolytes: (1) propylene carbonate (PC) and diethyl carbonate (DEC) (1:2 by weight) $1\,mol\,dm^{-3}$ $LiPF_6$; (2) ethylene carbonate (EC) and DEC (1:2 by weight) $1\,mol\,dm^{-3}$ $LiPF_6$. Characterization is performed by cyclic voltammetry, impedance spectroscopy, scanning electron microscopy (SEM), electrochemical impedance spectroscopy (EIS), X-ray photoelectron spectroscopy (XPS) and half cell tests. Cyclic life is better in either electrolyte with VC than either electrolyte with/without VTC. SEM shows VC and VTC both form well developed passivation films on the graphite anode, but the films with VTC are thicker than with VC. EIS shows the VTC films have significantly higher charge transfer resistance. The VTC film in PC fails to protect against exfoliation. XPS indicates VTC has different reaction pathways in PC relative to EC. In EC/DEC, VTC forms polymeric C–O–C-like components and sulfide species (C–S–S–C, S and C–S–C). In PC/DEC, VTC does not form polymeric species, instead forming a film mainly containing LiF and Li_2S. It appears that a thinner polymeric film is preferential. The specific data herein are of interest, and the general conclusions may help development of improved additives for enhanced Li-ion battery performance.

© 2011 Elsevier B.V. All rights reserved.

1. Introduction

In commercially available lithium-ion batteries, the lithium ion is electrochemically intercalated into the graphite negative electrode during charging and de-intercalated during discharging [1,2]. The transfer behavior of Li^+ across the interface between the anode material and the electrolyte depends greatly on the properties of the solid electrolyte interface (SEI) layer in terms of Li^+-conductivity, Li^+ transfer number, SEI stability, etc. The structure and performance of the SEI film formed on the graphite surface has been widely studied [3–6]. The SEI formation reactions are basically irreversible, but the irreversibility depends strongly on the electrolyte solution (including solvents, additives and salts). Alkyl carbonates such as propylene carbonate (PC), ethylene carbonate (EC), diethyl carbonate (DEC) and dimethyl carbonate (DMC) are among the most important solvents for electrolytes in lithium ion batteries because they are aprotic, polar and non-volatile. Use of PC-based electrolytes always results in exfoliation of graphite, electrolyte decomposition and liberation of organic gas in the battery [6]. Carbon materials have good cyclic life in EC/DEC electrolytes due to formation of a good passivation film on the carbon surface [7–10]. Zaghib et al. [9] reported that passivation film formation was not only due to solvent decomposition but was also affected by the salt in the EC/DEC system. In general, both solvent molecules and PF_6^- anions interact with lithium during first charge to form surface films composed of $ROCO_2Li$, $ROLi$ and Li_2CO_3 species containing Li–C bonds, polymeric species (e.g. polycarbonate, polyethylene), LiF, Li_xPF_y and Li_xPOF_y species [11]. Much research has been published on electrolyte additives because electrolyte additives participate in the formation of SEI films and can have critical effects on battery performance [12]. Many additives have been studied, for example CO_2 [13], N_2O [13], S_x^{2-} [13], SO_2 [14,15], chloroethylene carbonate [16], vinyl propylene carbonate [6], vinylene carbonate (VC) [6,17,18], vinyl acetate [6], 2,2-dimethoxy-propane [19], 1,3-propane sultone [20], tris(pentafluorophenyl) borane [21,22] and ethylene sulfite [6,23]. It is further reported that vinyl- and oxy-group additives such as VC can improve the cycle life and the reversible capacity of Li-ion batteries [6,17,18]. The main function of the vinyl-group is electrochemical polymerization with the SEI material on the graphite surface during SEI film formation. The oxy-groups, i.e. electron-withdrawing groups, function mainly as components of the SEI film, making the vinyl group more electrophilic and thus facilitating reduction. Although venylene trithiocarbonate (VTC) has been

* Corresponding author. Tel.: +886 62606123x7208; fax: +886 62602205.
E-mail address: ccchang@mail.nutn.edu.tw (C.-C. Chang).
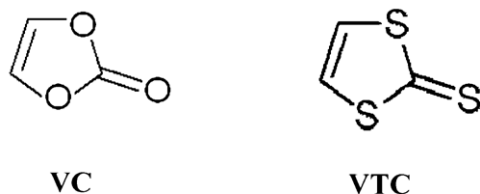
Scheme 1. The chemical structures of the VC and VTC additives.

patented by Matsushita Electric Industrial Co. [24], investigation of vinyl- and sulf-group compounds as electrolyte additives for Li-ion batteries has been scant.

This present study explores SEI behavior and mechanisms on a graphitic anode surface by comparing the differential effects of two different additives in two different solvents. VC and VTC are considered as electrolyte additives to liquid organic electrolyte for lithium ion cells. A PC-based solvent system is one of the two solvent systems, since PC is known to co-intercalate into graphitic layers with Li$^+$ and exfoliate graphitic carbon without formation of an effective SEI film [25]. We also explore an EC-based solvent system, which is representative of general commercial applications. [26] In fact, the employed electrolytes are mixed solvents of PC/DEC and EC/DEC. The anodes for typical Li-ion batteries involve carbon-based materials and are commonly categorized into three types, namely natural graphite, artificial graphite and graphite-like carbon. Natural graphite is superior to other carbon candidates for a number of reasons, e.g. high capacity, low irreversible capacity at first cycle, flat and low potential profile, numerous suppliers and low cost. Thus, natural graphite (NG) is selected as the anode material in this study.

The produced SEI films are characterized and the effects on electrochemical performance are investigated. Evaluations are performed by cyclic voltammetry, impedance spectroscopy, scanning electron microscopy (SEM), electrochemical impedance spectroscopy (EIS), X-ray photoelectron spectroscopy (XPS) and half cell tests.

2. Experimental

VC (Aldrich, >98%), VTC (Aldrich, >98%), hexafluorophosphate (LiPF$_6$, Kanto Denka Koyo Co. Ltd., battery grade), ethylene carbonate (EC, Ferro Corp., battery grade), propylene carbonate (PC, Ferro Corp., battery grade) and diethyl carbonate (DEC, Ferro Corp., battery grade) were stored under an argon atmosphere and used without further purification. The structures of the additives are shown in Scheme 1. Lithium foil was obtained from FMC Inc. Natural graphite (China Steel Chemical Corp.) was used as the active anode material. The electrolytes were prepared as two types: EC/DEC (1:2, w/w) and PC/DEC (1:2, w/w) with 1 mol dm^{-3} LiPF$_6$ with/without VC or VTC additives (3% by weight). These electrolytes were prepared in a glove box which contained less than 5 ppm of H$_2$O and O$_2$. The electrolytes contained less than 10 ppm of water and less than 50 ppm of hydrofluoric acid.

Test electrodes were prepared by mixing together Super P (3 wt%, MMM Carbon, Belgium), NG (90 wt%), a polyvinylidenedifluoride powder polymer binding agent (7 wt%, PVDF Solef 6020, Solvy) and the solvent N-methylpyrrolidinone (NMP, ISP) to form a slurry. The mixed slurry was coated onto copper foil (10 μm, Nippon Foil Co., Japan) and dried at 90 °C. The dried electrodes were compressed by a roller at room temperature to make a smooth and compact structure. The electrodes were inspected for uniform surface. Electrodes of similar surface area, thickness and weight were selected for further testing. Finally, to remove residual water content and standardize the level of hydration, the selected electrodes were stored in a glove box with oxygen and humidity content

maintained below 5 ppm for more than 24 h before electrochemical characterization.

Electrochemical performance of the additives was investigated by use of a two-electrode test cell (2032 coin-type cell) which consisted of an NG anode, a microporous separator (Celgard 2300), a metallic lithium electrode and an electrolyte. Coin-type cells for testing were assembled in a glove box. Lithium sheet (FMC) of 0.2 mm thickness was cut into disk shapes for use as negative electrodes. Test cells were evaluated for charge/discharge behavior under constant current conditions, cycled galvanostatically at 0.1C (0.325 mA cm^{-2}) over the range of 0.003–1.8 V.

Cyclic voltammetry (CV) measurements were carried out with an Autolab electrochemical analyzer (Autolab PGSTAT30, Eco Chemie) with a current sensitivity of 1 nA. A one-compartment three-electrode cell was used, with the whole apparatus set in a glove box. The working electrode was an NG electrode prepared by the above procedure with a dimension of 1×1 cm^2. Both the counter and the reference electrodes were lithium metal. After cyclic voltammetric measurement, electrochemical impedance spectroscopy was observed immediately at fully charged (i.e. fully lithiumed, voltage at ca. 0.01 V) conditions. EIS was performed in a batch reactor by coupling the potentiostat with an Autolab frequency response analyzer and an impedance phase analyzer. A sinusoidal amplitude modulation of ±10 mV was used over a frequency range of 0.01–10^6 Hz.

Surface morphology of the composite electrode was evaluated by SEM (Joel JSM35, 20 kV). Surface composition analysis of the anode surface was performed by XPS (ESCA 210, V. G. Scientific Limited). The analyzed area of the samples was 100 μm × 100 μm. The binding energy scale was calibrated from the graphite using the C 1s peak at 284.3 eV.

3. Results and discussion

3.1. Half cell performance test

To determine the contributions of the additives to cycleablility, 3 wt% of VC or VTC was added to electrolytes of 1 mol dm^{-3} LiPF$_6$ dissolved in: (1) PC/DEC (1/2, w/w); (2) EC/DEC (1/2, w/w). For reference, comparable coin-type without any additive were also fabricated.

Results of the cyclic experiments are summarized in Fig. 1. It is seen that the VC additive produces better cyclic performance than the VTC. With VC, the PC-based electrolyte maintains good cycling performance due to formation of a good passivation film
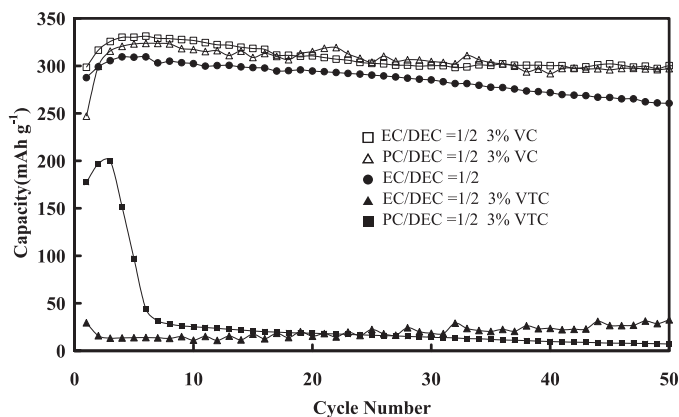

Fig. 1. Cycle life performance of natural graphite. Electrolyte with 1 mol dm^{-3} LiPF$_6$ in solvents: (□) PC/DEC = 1:2 (by weight) 3 wt% VC, (■) PC/DEC = 1:2 (by weight) 3 wt% VTC, (●) EC/DEC = 1:2 (by weight), (□) EC/DEC = 1:2 (by weight) 3 wt% VC, (▲) EC/DEC = 1:2 (by weight) 3 wt% VTC.
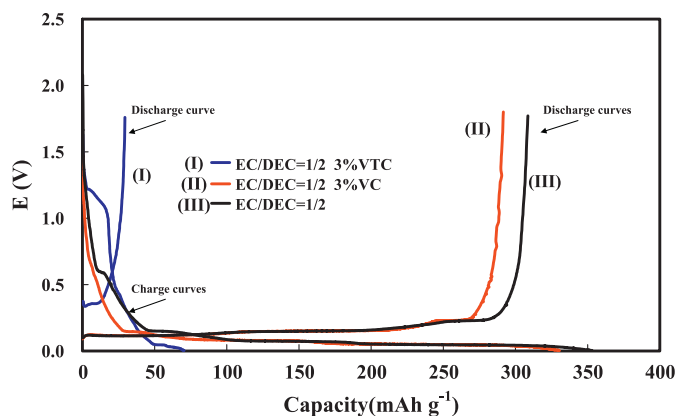
Fig. 2. Charge and discharge capacity at 0.1 C in the first cycle of graphite electrode using 1 mol dm^{-3} LiPF$_6$ in EC/DEC (1:2 by weight) with/without 3 wt% VC or VTC.

[17,27,28]. The EC-based electrolyte without additive also maintains good cycling performance, likewise due a good passivation film [7–10]. In contrast, the discharge capacity with VTC in EC/DEC is very low (around 25 mA h g^{-1}). The discharge capacity decreases after the third cycle but then increases slightly with increasing cycle number. This indicates that the SEI formed by VTC in EC/DEC has high resistance to Li$^+$ transfer. In the PC-based electrolyte, the cell with no additive does not cycle at all due to PC solvent co-intercalation with Li$^+$ into the graphite and exfoliation of graphitic carbon because of lack of an effective SEI film [25]. The discharge capacity in PC/DEC with VTC remains around 200 mA h g^{-1} and then quickly decreases after the third cycle. This suggests that VTC helps form an SEI, but the produced SEI does not protect from exfoliation.

Figs. 2 and 3, respectively, show the first charge/discharge (formation cycle) capacities at a rate of 0.1C for the graphite/Li cells with EC/DEC or PC/DEC electrolytes and VC or VTC additive. The charge/discharge curves in Fig. 2 reveal that, over the 1.5–0.2 V range, less SEI is formed in EC/DEC with VC than in EC/DEC either without or with VTC. This indicates that the VC additive forms a thinner SEI. Further, the VTC additive decomposes at around 1.3 V but maintains a shoulder around 16 mA h g^{-1}, after which the voltage drops rapidly to 0.003 V. This indicates that the SEI film formed in EC/DEC with VTC, compared to the VC case, has a higher resistance to Li$^+$ transfer. Thus, the discharge behavior in EC/DEC with VTC shows a higher starting voltage (approx. 0.32 V) and lower capacity. From the charge curves of Fig. 3, it can be seen that the VC additive also shows good SEI formation. In contrast, the PC/DEC electrolyte without additive fails to form an effective SEI
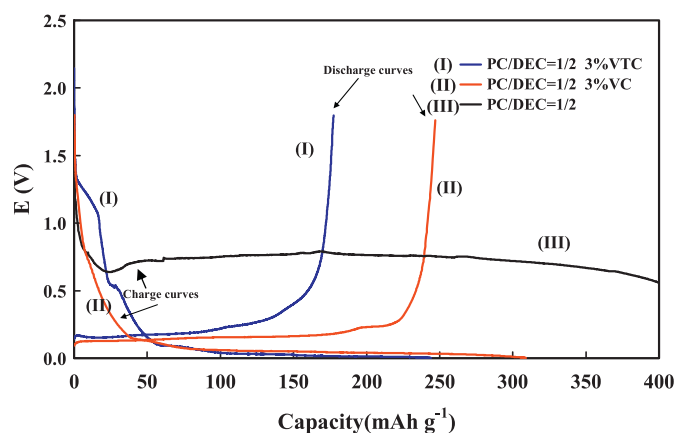

Fig. 3. Charge and discharge capacity at 0.1C in the first cycle of graphite electrode using 1 mol dm^{-3} LiPF$_6$ in PC/DEC (1:2 by weight) with/without 3 wt% VC or VTC.

film around 0.77 V and thus continues to exfoliate graphitic carbon. Further, it is seen that the VTC additive decomposes around 1.3 V and shows SEI formation around 16 mA h g^{-1}, both values being similar to the VTC case. The discharge capacities of VC and VTC in PC/DEC are 250 and 177 mA h g^{-1}, respectively. The VTC additive appears to form a SEI film which protects slightly against graphite exfoliation at first charge. The discharge capacity performances are assumed to reflect the different SEI films which form in the PC or EC solvents with/without VC or VTC addition. Based on this assumption, it can be concluded that VC forms a better SEI than VTC. The above data indicate that 3 wt% VC added to either EC-based or PC-based electrolytes exhibits improve half cell discharge in Li-ion batteries.

3.2. Surface morphology

The surface morphology of a graphite anode is critical to formation of an SEI. Thus the surface morphologies of the NG anodes under the various electrolyte/additive conditions after third cycle 0.1 C charge–discharge are examined SEM (Fig. 4). The NG surface in PC/DEC without additive is clearly exfoliated and displays no SEI, as seen in Fig. 4(a). When either electrolyte containing either additive is considered, the anodes are completely covered with an SEI film, as seen in Fig. 4(b and d–f). Interestingly, the morphologies for the VC-containing electrolytes (Fig. 4(b and e) display SEI films that are much thinner than the VTC-containing electrolytes. This agrees with the fact that the cycleabilities in both PC/DEC and EC/DEC with VC and also in EC/DEC without additive are excellent. Fig. 4(c and f) display the SEI formed on NG in PC- and EC-based electrolytes respectively, both with VTC additive. It is seen in these micrographs that the NG is heavily coated with a layer of pulpy film, displaying net morphologies that are quite different than those in Fig. 4 (b, d and e). In the other words, PC/DEC or EC/DEC with VTC produces the thickest SEI, whereas PC/DEC or EC/DEC with VC produces the thinnest SEI. Further, the SEI of PC/DEC with VTC does not prevent exfoliation by PC co-intercalation into graphite layer, resulting in the degraded but SEI-covered NG morphology of Fig. 4(c).

3.3. Electrochemical test

The mechanisms whereby VC helps SEI formation have been considered in several prior studies [27–30]. In the following, SEI formation mechanisms are considered for EC/DEC and PC/DEC with VTC. The characteristics of the SEI are explored by cyclic voltammetry and electrochemical impedance spectroscopy.

The cyclic voltammograms of the NG electrode in 1 mol dm^{-3} LiPF$_6$ dissolved in EC/DEC (1:2 by w/w) without/with 3 wt% VTC additive are shown in Fig. 5(a and b), respectively. Examination of curve (I) in Fig. 5(a) shows a broad intense peak starting around 0.90 V and centered curve 0.75 V, presumably corresponding to the formation of a passivating SEI film [31]. During the first reduction of graphite in EC/DEC with VTC, three peaks are observed (1.35 V, 1.0 V and 0.0 V (vs. Li$^+$/Li)). The peak at 1.35 V decreases with further cycling (Fig. 5(b) curves (II) and (III)). This phenomenon is attributed to the irreversible reduction of VTC at the electrode surface. The 1.0 V peak disappears completely with further cycling (Fig. 5(b) curves (II) and (III)). This phenomenon is likewise attributed to irreversible reduction of VTC. The peak at 0.75 V is attributed to EC decomposition [32]. This peak disappears when VTC is added to the electrolyte. The reduction current at 0.0 V with VTC is lower than without VTC. The relative reduction current represents the intercalation of Li$^+$ into the graphite at 0.0 V. These results indicate that the SEI film formed in the EC/DEC electrolyte with VTC has a larger Li$^+$ transfer resistance than the SEI film formed without the additive.
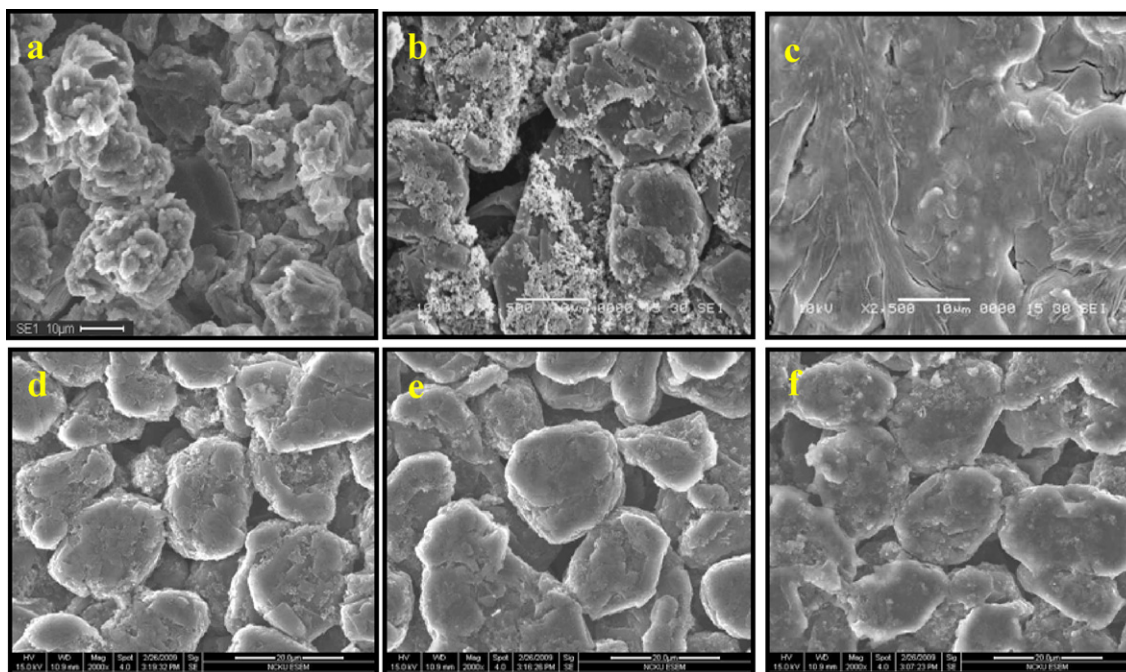
Fig. 4. SEM image after 0.1C charge/discharge 3 cycles. Electrolyte with 1 mol dm^{-3} LiPF$_6$ in solvents: (a) PC/DEC = 1:2 (by weight), (b) PC/DEC = 1:2 (by weight) 3 wt% VC, (c) PC/DEC = 1:2 (by weight) 3 wt% VTC, (d) EC/DEC = 1:2 (by weight), (e) EC/DEC = 1:2 (by weight) 3 wt% VC, (f) EC/DEC = 1:2 (by weight) 3 wt% VTC.

Cyclic voltammograms of the NG electrodes in 1 mol dm^{-3} LiPF$_6$ dissolved in PC/DEC (1:2 by w/w) without/with 3 wt% VTC are seen in Fig. 6(a and b), respectively. Although PC is an attractive electrolyte component in Li-ion batteries because of physical properties

such as low viscosity, high boiling point and high electric constant, Fig. 6(a) shows that PC does not form an adequate passivation film on NG. The graphite exfoliates (Fig. 4(a)) due to cointercalation and PC decomposition [6]. During the first reduction in EC/DEC with
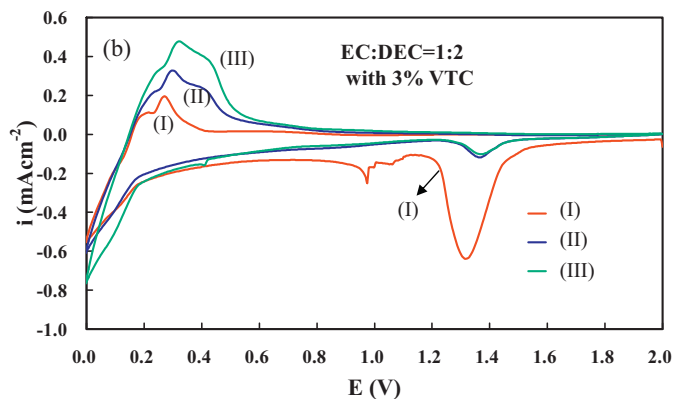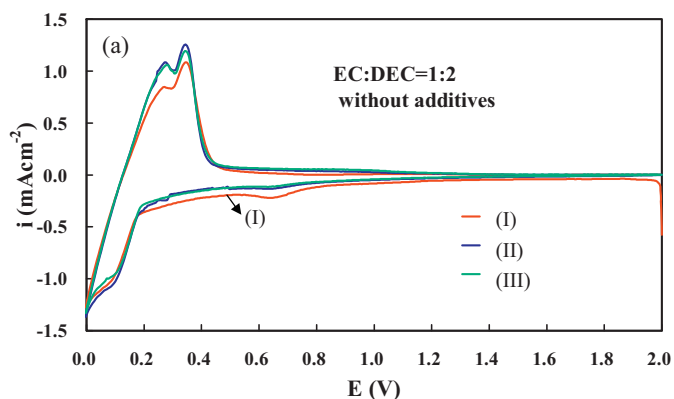

Fig. 5. Cyclic voltammograms of graphite in electrolyte with 1 mol dm^{-3} LiPF$_6$ in solvents: (a) EC/DEC = 1:2 (by weight), (b) EC/DEC = 1:2 (by weight) 3 wt% VTC. (I) = first cycle, (II) = second cycle, (III) = third cycle.
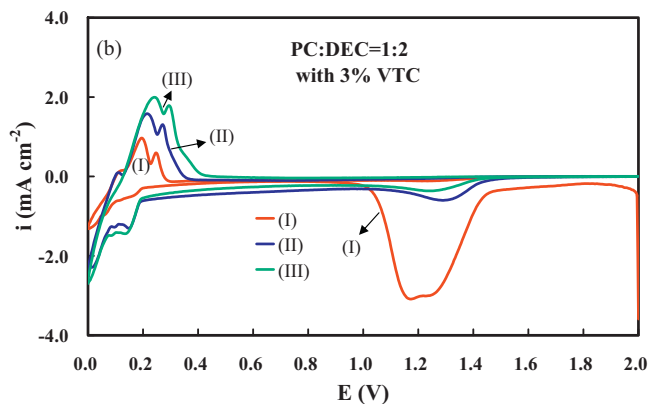

Fig. 6. Cyclic voltammograms of graphite in electrolyte with 1 mol dm^{-3} LiPF$_6$ in solvents: (a) PC/DEC = 1:2 (by weight), (b) PC/DEC = 1:2 (by weight) 3 wt% VTC. (I) = first cycle, (II) = second cycle, (III) = third cycle.
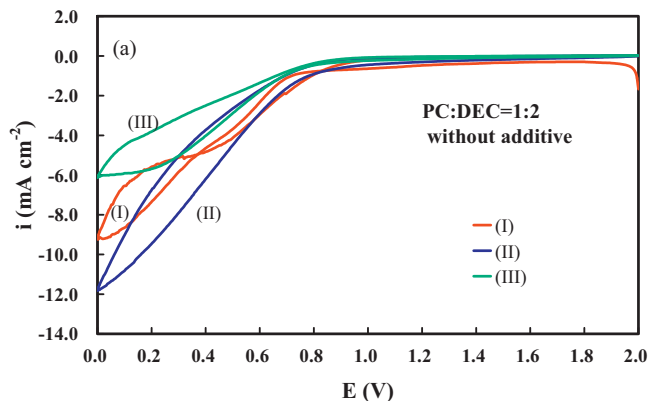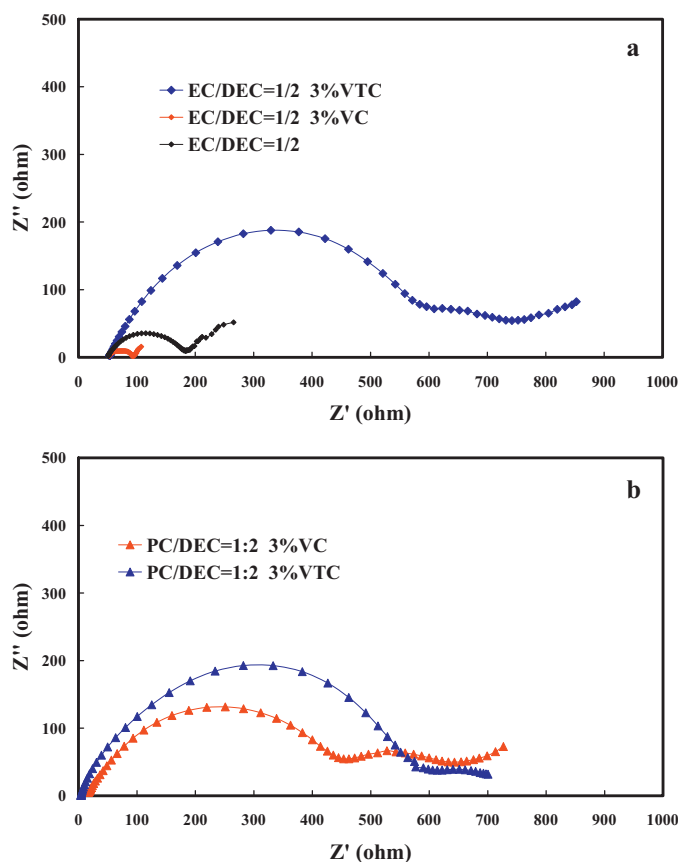
Fig. 7. Impedance spectra of fully discharged graphite electrodes in electrolyte with 1 mol dm^{-3} LiPF$_6$ with/without 3 wt% VC or VTC: (a) EC/DEC = 1:2 (by weight); (b) PC/DEC = 1:2 (by weight). Frequency range: 0.01 Hz to 10^6 Hz.

VTC (curve (I), Fig. 6(b)), peaks are observed at 1.25 V, 0.2 V and 0.0 V (vs. Li$^+$/Li). The 1.25 V peak decreases with further cycling (Fig. 6(b), curves (II) and (III)). This is attributed to irreversible reduction of VTC and consequently reduced VTC concentration at the electrode surface. However, the peak at 0.75 V caused by PC decomposition disappears when VTC is added to the electrolyte. The 0.2 V and 0.0 V peaks also decrease due to the high Li$^+$ transfer resistance of the thick SEI film formed by VTC in PC/DEC.

It is well known that electrochemical impedance spectroscopy can detect the Li$^+$ conductivity of an SEI film, with lower EIS impedance values indicating faster Li$^+$ transport. Accordingly, EIS impedance is measured immediately after CV scan. The impedance spectra of the EC/DEC and PC/DEC electrolytes with the two additives are shown in Fig. 7(a and b), respectively. The figures show higher impedance values in the VTC case, implying sluggish Li$^+$ movement through the VTC-derived SEI, presumably contributing to capacity loss during cycling. In contrast, the SEI films of EC/DEC alone and EC/DEC with VC show low impedance and low thickness values (thickness determined by impedance values and SEM results). Consequently, the EC/DEC cells without/with VC demonstrate superior cycleability. The cell containing VC shows the lowest impedance value, even compared to the electrolyte without additive. Clearly, the SEI components play a critical role in the electrochemical performance.

3.4. XPS analysis of SEI

XPS has been used to study SEI composition and chemical bonding states of [28,33–35]. Although XPS analysis is limited by the escape depth of the electrons, usually about 3–5 nm, this is suitable

for studying surface films. To analyze the composition and chemical bonding states of the SEI formed in this study, XPS is performed on the NG anode after the third cycle and full discharge for the PC-based and EC-based electrolytes with 3 wt% VTC. Fig. 8 shows the C 1s, O 1s, F 1s and S 2p spectra of the NG electrode in 1 mol dm^{-3} LiPF$_6$ EC/DEC (1:2 by weight) with/without 3 wt% VTC and PC/DEC (1:2) with 3 wt% VTC.

C 1s core peak: The C 1s spectrum of the graphite in the different electrolytes (Fig. 8, C 1s) consists of a number of peaks. For example, the peak at 284.3 eV corresponds to graphite; the peak at 282.5–283 eV corresponds to LiC$_x$-like environments (e.g. Li$_2$C$_2$, LiC$_6$); 285.8–289 eV corresponds to CO-like environments (e.g. (CH$_2$OCO$_2$)$_2$Li$_2$); 289–291 eV corresponds to CO$_3$-like environments (e.g. ROCO$_2$Li) [27,34,36,37]. The intensities of the CO$_3$-like components at the 289–291 eV peak in the EC/DEC electrolyte without VTC are more pronounced than those in the EC/DEC and PC/DEC electrolytes with 3 wt% VTC. The intensity of C–O–C-like component at 286.5 eV for EC/DEC with 3 wt% VTC is stronger than for EC/DEC without VTC and for PC/DEC with 3 wt% VTC. The intensity of the LiC$_x$-like component at 283 eV for PC/DEC with 3 wt% VTC is larger than for EC/DEC without VTC and for EC/DEC with 3 wt% VTC. The LiC$_x$-like component is attributed to exfoliation by PC-cointercalation into the graphite. These results indicate that VTC enhances SEI formation on the NG surface. The results also indicate that VTC undergoes different reactions with PC than with EC. VTC in EC/DEC forms polymeric C–O–C-like components, whereas VTC in PC/DEC does not readily form such polymeric species. The occurrence of these polymeric C–O–C-like components correlates with greater protection of the NG electrode from exfoliation. *O 1s core peak*: The O 1s spectrum of the graphite in the different electrolytes (Fig. 8, O 1s) consists of a number of peaks. For example, the peak at 528–530 eV corresponds to Li–O-like environments (e.g. Li$_2$O and Li–O–C); the peak at 531–534 eV corresponds to –C=O, C–O–C environments (e.g. Li$_2$CO$_3$, ROCO$_2$Li, polyethylenecarbonate) [27,34,36,37]. The intensity of the Li-O-like component at 528–530 eV for PC/DEC with 3 wt% VTC is greater than for EC/DEC without VTC and EC/DEC with 3 wt% VTC. The intensity of the C–O–C-like component at 533.5 eV for EC/DEC with 3 wt% VTC is greater than that for EC/DEC without VTC and PC/DEC with 3 wt% VTC. These results indicate that PC/DEC with 3 wt% VTC readily forms Li$_2$O and Li$_2$CO$_3$ but does not form C–O–C-like components or polyethylenecarbonate on the graphite surface. Again it is seen that VTC interacts differently with PC than with EC, and that the PC/DEC solvent does not easily form the polymeric species which appear to protect the graphite surface from exfoliation in a PC solvent.

F 1s and S 2p core peaks: The F 1s spectrum (Fig. 8, F 1s) shows two main peak regions. The first region at 684.8–686.4 eV is attributed to LiF, which is a degradation product of LiPF$_6$ [27,34,36,38]. The second region at 688 eV is attributed to C–F of PVDF (polyvinylidenedifluoride, a binder in the electrode) [36]. The intensity of the LiF component at 684.8–686.4 eV for PC/DEC with VTC is greater than for EC/DEC without VTC and EC/DEC with VTC. This indicates that the SEI films formed in PC/DEC with VTC have larger resistance to electron and Li$^+$ transfer. The S 2p spectrum of the graphite in the different electrolytes (Fig. 8, S 2p) consists of two main peak regions. The region at 160.8–163 eV is attributed to Li$_2$S [39], which is a VTC degradation product. The second region at 163.6–165 eV corresponds to sulfide species such as C–S–S–C, S and C–S–C [30,40]. The peak at 164.5 eV is considered to be reduced sulfur [41]. The intensity of the L$_2$S component at 160.8–163 eV for PC/DEC VTC is stronger than for EC/DEC with VTC. The intensity of the 163.6–165 eV sulfide species is stronger for EC/DEC with VTC than for PC/DEC with VTC. The data indicating that the SEI on the graphite anode contains alkyl sulfide species is, to our knowledge, a new observation and can help explain SEI
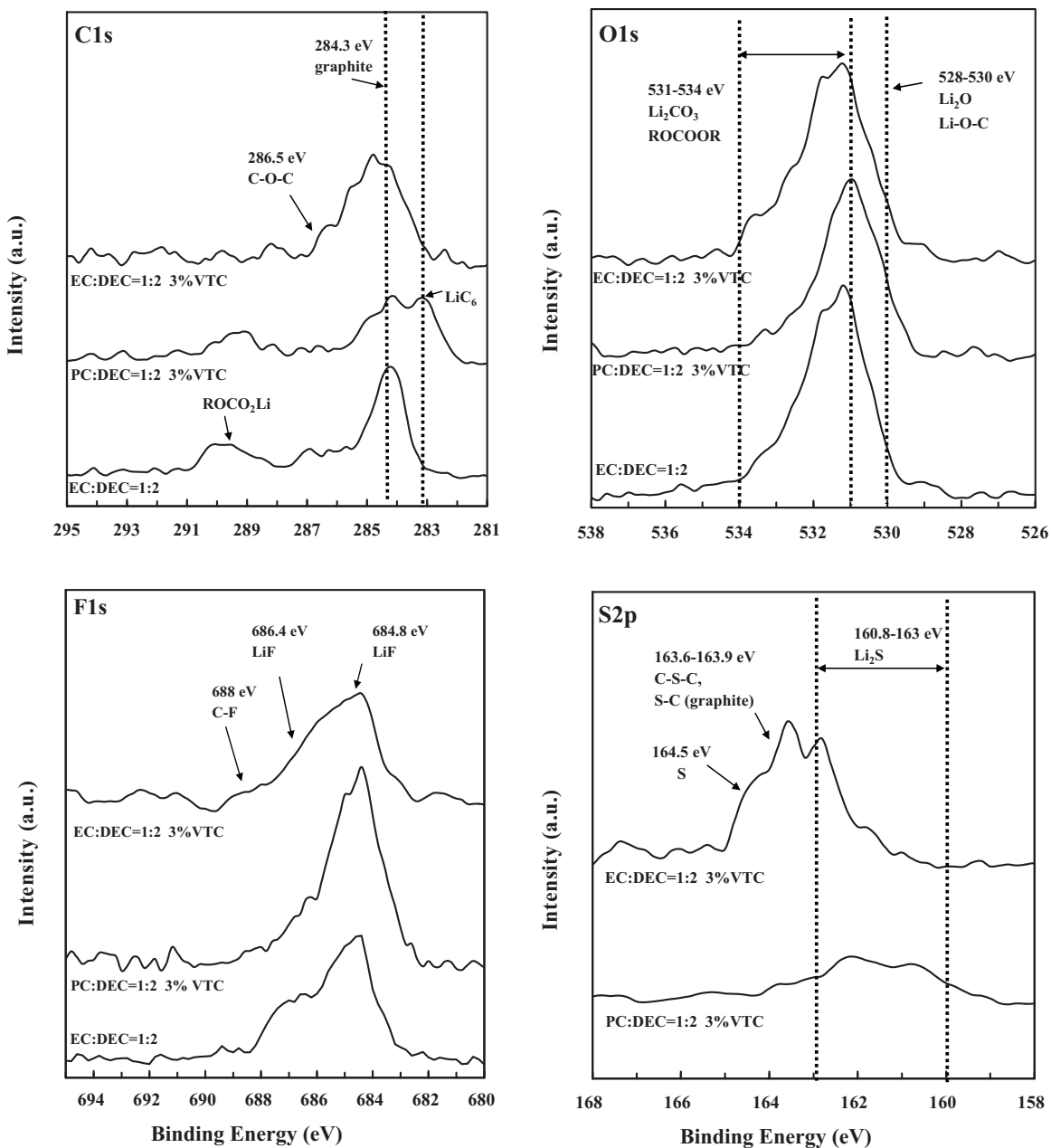
Fig. 8. C 1s, O 1s, F 1s and S 2p XPS spectra of graphite anodes after 3rd cycle.

formation in various solvents. The SEI for the electrolytes with VTC are further investigated based on the different S oxidation states. It is found that the SEI contains sulfite compounds such as inorganics like Li_2S (a major species in PC/DEC electrolyte) and organics like C–S–S–C, S and C–S–C (major species in EC/DEC electrolyte).

The combined results SEM EIS, half cell testing and CV results show that both VC or VTC additives in both electrolytes form SEI films on a NG surface. However, VTC forms a thicker SEI than VC, and has higher Li^+ transfer resistance. XPS shows that VTC follows different reaction pathways in PC- verses EC-based solvents. In EC/DEC, VTC forms C–O–C-like and sulfide components (C–S–S–C, S and C–S–C), whereas VTC in PC/DEC forms predominantly LiF and Li_2S components, without polymeric species. The VTC/PC/DEC SEI does not prevent NG exfoliation. A thinner polymeric SEI is seems preferential.

4. Conclusion

In this study, electrochemical impedance spectroscopy, cyclic voltammetry, half cell tests, scanning electron microscopy and X-ray spectroscopy were employed to investigate and compare VC and VTC as additives in EC/DEC or PC/DEC electrolyte for Li-ion batteries. SEM EIS, half cell testing and CV results showed that both additives in both electrolytes formed SEI films on the NG surface. However, the SEI produced with VTC were thicker than those formed with the VC additive and had higher Li^+ transfer resistance. XPS results showed that VTC followed different reaction pathways in the PC-based verses EC-based solvents. In EC/DEC, VTC formed C–O–C-like components and sulfide species (C–S–S–C, S and C–S–C), but in PC/DEC VTC formed predominantly LiF and Li_2S, and did not easily form polymeric species. The SEI of VTC in PC/DEC did not protect NG exfoliation. It appears that a thinner polymeric

SEI is preferential. The specific data herein are of interest, and the general conclusions may help development of improved additives for enhanced Li-ion battery performance.

Acknowledgements

References

[1] M. Winter, P. Novak, A. Monnier, J. Electrochem. Soc. 145 (1998) 428.
[2] T. Nakajima, J. Fluorine Chem. 105 (2000) 229.
[3] D. Aurbach, A. Zaban, Y. Ein-Eli, I. Weissman, O. Chusid, B. Markovsky, M. Levi, E. Levi, A. Schechter, E. Granot, J. Power Sources 68 (1997) 91.
[4] O. Chusid, Y. Ein-Eli, D. Aurbach, M. Babai, Y. Carmeli, J. Power Sources 43–44 (1993) 47.
[5] D. Aurbach, M. Levi, E. Levi, A. Schechter, J. Phys. Chem. B 101 (1997) 2195.
[6] K. Abe, H. Yoshitake, T. Kitakura, T. Hattori, H. Wang, M. Yoshio, Electrochim. Acta 49 (2004) 4613.
[7] K. Tatsumi, K. Zaghib, H. Abe, S. Higuch, T. Ohsaki, Y. Sanade, J. Power Sources 54 (1995) 425.
[8] H. Abe, K. Zaghib, K. Tatsumi, S. Higuchi, J. Power Sources 54 (1995) 236.
[9] K. Zaghib, K. Tatsumi, H. Abe, T. Ohsaki, Y. Sawada, S. Higuchi, J. Power Sources 54 (1995) 435.
[10] G. Li, R. Xue, L. Chen, Y. Huang, J. Power Sources 54 (1995) 271.
[11] D. Aurbach, E. Zingigrad, Y. Cohen, H. Teller, Solid State Ionics 148 (2002) 405.
[12] E. Peled, D. Golodnitsky, G. Adriel, J. Electrochem. Soc. 144 (1997) 823.
[13] J.O. Besenhard, M.W. Wagner, M. Winter, A.D. Jannakoudakis, P.D. Jannakoudakis, E. Theodoridou, J. Power Sources 43–44 (1993) 413.
[14] J.D. Besenhand, M. Winter, J. Yang, W. Biberacher, J. Power Sources 54 (1995) 228.
[15] Y. Ein-Eli, S.R. Thomas, V.R. Koch, J. Electrochem. Soc. 142 (1997) 1159.
[16] Z.X. Shu, R.S. McMillan, J.J. Murray, J. Electrochem. Soc. 142 (1995) L161.
[17] H.-C. Wu, C.-Y. Su, D.-T. Shieh, M.-H. Yang, N.-L. Wu, Electrochem. Solid-State Lett. 9 (2006) A537.
[18] D. Aurbach, J.S. Gnanaraj, W. Geissler, M. Schmidt, J. Electrochem. Soc. 151 (2004) A23.
[19] C.C. Chang, L.J. Her, L.C. Chen, Y.Y. Lee, S.J. Liu, H.J. Tien, J. Power Sources 163 (2007) 1059.
[20] T. Hamamoto, A. Hitaka, Y. Nakada, K. Abe, U.S. Patent 6,033,809, 1998.
[21] C.C. Chang, T.K. Chen, J. Power Sources 193 (2009) 834.
[22] C.C. Chang, T.K. Chen, L.J. Her, G.T.K. Fey, J. Electrochem. Soc. 156 (2009) A828.
[23] G.H. Wrodnigg, J.O. Besenhard, M. Winter, J. Electrochem. Soc. 146 (1999) 470.
[24] K. Iwamoto, T. Oura, K. Sonoda, M. Hatazaki, H. Yoshizawa, S. Nakanishi, U.S. Patent 6,958,198, 2005.
[25] M. Yoshio, H. Wang, K. Fukuda, Y. Hara, Y. Adachi, J. Electrochem. Soc. 147 (2000) 1245.
[26] D. Aurbach, M.L. Daroux, P.W. Faguy, E. Yeager, J. Electrochem. Soc. 134 (1987) 1611.
[27] L.E. Ouatani, R. Dedryvère, C. Siret, P. Biensan, S. Reynaud, P. Iratcabal, D. Gonbeau, J. Electrochem. Soc. 156 (2009) A103.
[28] M. Lu, H. Cheng, Y. Yang, Electrochim. Acta 53 (2008) 3539.
[29] T. Sasaki, T. Abe, Y. Iriyama, M. Inaba, Z. Ogumi, J. Electrochem. Soc. 152 (2005) A2046.
[30] K. Tasaki, K. Kanda, T. Kobayashi, S. Nakamura, M. Ue, J. Electrochem. Soc. 153 (2006) A2192.
[31] A. Dailly, J. Ghanbaja, P. Willmann, D. Billaud, Electrochim. Acta 48 (2003) 977.
[32] M.E. Spahr, D. Goers, W. Märkle, J. Dentzer, A. Würsig, H. Buqa, C. Vix-Guterl, P. Novák, Electrochim. Acta 55 (2010) 8928.
[33] Y.S. Hu, W.H. Kong, H. Li, X.J. Huang, L.Q. Chen, Electrochem. Commun. 6 (2004) 126.
[34] P. Verma, P. Maire, P. Novák, Electrochim. Acta 55 (2010) 6332.
[35] S.H. Kang, D.P. Abraham, A. Xiao, B.L. Lucht, J. Power Sources 175 (2008) 526.
[36] H. Ota, Y. Sakata, A. Inoue, S. Yamaguchi, J. Electrochem. Soc. 151 (2004) A1659.
[37] D. Aurbach, I. Weissman, A. Schechter, H. Cohen, Langmuir 12 (1996) 3991.
[38] Y. kawamoto, K. Ogura, M. Shojiya, M. Takahashi, K. Kadono, J. Fluorine Chem. 96 (1999) 135.
[39] H. Cheng, C. Zhu, M. Lu, Y. Yang, J. Power Sources 173 (2007) 531.
[40] B.J. Linderg, K. Hamrin, G. Johansson, V. Gelius, A. Fahlmann, C. Nordling, K. Siegbahn, Phys. Scripta 1 (1970) 286.
[41] H. Ota, T. Akai, H. Namita, S. Yamaguchi, M. Nomura, J. Power Sources 119–121 (2003) 567.